Journal of Alloys and Compounds 682 (2016) 825–831

Contents lists available at ScienceDirect

Journal of Alloys and Compounds

journal homepage: http://www.elsevier.com/locate/jalcom

Critical behavior study of $Pr_{1-x}Sr_xMnO_3$ and $Nd_{1-x}Sr_xMnO_3$ with $x = 1/2$

A. Oleaga [a, *], A. Salazar [a], M. Ciomaga Hatnean [b], G. Balakrishnan [b]

[a] Departamento de Física Aplicada I, Escuela Técnica Superior de Ingeniería, Universidad del País Vasco UPV/EHU, Alameda Urquijo s/n, 48013 Bilbao, Spain
[b] Department of Physics, University of Warwick, Coventry CV4 7AL, UK

ARTICLE INFO

Article history:
Received 16 March 2016
Received in revised form
27 April 2016
Accepted 28 April 2016
Available online 9 May 2016

Keywords:
Manganites
Critical behavior
Universality class
Ferromagnetism

ABSTRACT

Magnetic measurements have been performed on single crystalline samples of $Pr_{0.5}Sr_{0.5}MnO_3$ and $Nd_{0.5}Sr_{0.5}MnO_3$ to develop a complete critical behavior study of the paramagnetic to ferromagnetic transition in both manganites, which share many common features in their phase diagrams. The critical exponents β, γ and δ have been independently obtained. For $Pr_{0.5}Sr_{0.5}MnO_3$ these are $\beta = 0.376$, $\gamma = 1.403$ and $\delta = 4.72$ which are in close agreement with the 3D-Heisenberg model ($\beta = 0.365$, $\gamma = 1.386$ and $\delta = 4.80$) while for $Nd_{0.5}Sr_{0.5}MnO_3$ they are $\beta = 0.323$, $\gamma = 1.201$, and $\delta = 4.77$, which correspond to the 3D-Ising universality class ($\beta = 0.3265$, $\gamma = 1.237$ and $\delta = 4.79$). Magnetocrystalline anisotropies in $Nd_{0.5}Sr_{0.5}MnO_3$ are strong enough so that the magnetic transition is not compatible with the double exchange description while in $Pr_{0.5}Sr_{0.5}MnO_3$ they are not so relevant; in this last case the isotropic description is of application.

1. Introduction

Half-doped manganites $R_{0.5}Sr_{0.5}MnO_3$ (R = Pr, Nd) are specially interesting due to their colossal magnetoresistance (CMR) together with their particular phase diagram with respect to other doping concentrations. From room temperature (where they are both in a paramagnetic insulator state) downwards, a ferromagnetic metallic phase (FM) is developed at about 250K while at lower temperature they both become antiferromagnetic insulators (AFM) [1,2]. If CMR were simply described by the double exchange mechanism (DE), it would be expected that the system in the pure ferromagnetic metallic state had no orbital ordering and showed an isotropic behavior. But the study of the spin dynamics of these materials by neutron scattering measurements has shown the existence of the static $d_{x^2-y^2}-$ type orbital-ordering in both the paramagnetic and ferromagnetic states [3], implying that there is an anisotropic behavior which has been confirmed in the spin wave dispersion in the FM state. Besides, the antiferromagnetic ordering is different in these two manganites: it is the CE-type AFM spin structure accompanied with charge ordering for $Nd_{0.5}Sr_{0.5}MnO_3$ while it is the A-type for $Pr_{0.5}Sr_{0.5}MnO_3$ with the $d_{x^2-y^2}-$ type orbital order, without traces of charge ordering [4,5]. This difference is attributed to the widening of the one-electron bandwidth W in the case of the Pr compound with respect to the Nd one.

The phase diagram is even a little more complex for the case of $Nd_{0.5}Sr_{0.5}MnO_3$ as it has been demonstrated that there is a coexistence of an A-type antiferromagnetic phase with the CE-type below T_N using different techniques [1,4,6,7] and that there is also a coexistence of AFM phase in the FM region (between T_C and T_N) [6,8,9]. Concerning this last proposed phase coexistence, Kawano-Furukawa et al. found A-type AFM spin wave excitations in the FM state, which they attributed to a canted AFM ordering instead of a phase coexistence [3]. In the case of $Pr_{0.5}Sr_{0.5}MnO_3$, only some structural phase coexistence has been found at low temperature, starting below 148K [10].

The study of the critical behavior of the second order magnetic phase transitions is another valuable tool to study the appropriateness of the DE mechanism to describe the magnetism of the compounds. It has been theoretically shown that the 3D-Heisenberg model (which is isotropic) is compatible with the DE mechanism [11]; in the cases in which this mechanism does not describe well the magnetism of the transition because there are some other effects to be taken into account, the critical behavior will be described by other universality classes as the Hamiltonian which would describe the physics should contain new or coupling terms which could provoke a deviation from the isotropic case. The

* Corresponding author.
E-mail address: alberto.oleaga@ehu.es (A. Oleaga).

http://dx.doi.org/10.1016/j.jallcom.2016.04.315
0925-8388/

universality classes are characterized by a different set of critical exponents, whose particular values have been predicted by several mathematical methods [12–16].

In particular, the magnetic critical exponents β, γ and δ are associated to the spontaneous magnetization (M_S), the inverse of the initial susceptibility (χ_0^{-1}) and the critical isotherm ($M(H)$ at $T = T_C$), respectively. They fulfill the following equations in the near vicinity of the critical temperature T_C, written as a function of the reduced temperature $t = (T-T_C)/T_C$:

$$M_S(T) \sim |t|^{-\beta} \quad (T < T_C), \tag{1}$$

$$\chi_0^{-1}(T) \sim |t|^{\gamma} \quad (T > T_C), \tag{2}$$

$$M(H) \sim H^{1/\delta} \quad (T = T_C). \tag{3}$$

Lastly, the magnetic equation of state in the critical region is given by

$$M(H,t) = |t|^{\beta} f_{\pm}\left(H \Big/ |t|^{\beta+\gamma}\right) \tag{4}$$

where f_- and f_+ are regular analytic functions for $T < T_C$ and $T > T_C$, respectively.

And the following scaling laws give the relations among the critical exponents

$$\delta = 1 + \gamma/\beta \tag{5}$$

$$\alpha + 2\beta + \gamma = 2 \tag{6}$$

where α is the critical exponent associated to the specific heat

$$c_p(T) \sim A^{\pm}|t|^{-\alpha} \quad \left(A^- \text{ for } T < T_C,\ A^+ \text{ for } T > T_C\right) \tag{7}$$

and $A^{\pm}$ are the critical coefficients, whose ratio A^+/A^- is also theorized for each universality class. Table 1 contains the value of those critical exponents for the universality classes most commonly found in magnetic systems. There are some other critical exponents related to some other physical magnitudes which are scarcely evaluated but which also have particular values for the different universality classes.

The critical behavior of the ferromagnetic and antiferromagnetic transitions in manganites $R_{1-x}A_xMnO_3$ (R = rare earth, A = divalent cation) or even with a small co-doping is a broad field of study, with many published papers studying the features of particular compositions but where a systematic study is still pending. So far, the mean-field model (long-range interactions), the 3D-Heisenberg (short-range isotropic), the 3D-Ising (short-range uniaxial), 3D-XY (short-range planar) and even 2D models have been found to be of application depending on the particular sample, if the critical parameters obtained corresponded to a known universality class [17–31].

One of the drawbacks of many studies performed is that they have been done on polycrystalline samples, where it is much more difficult to extract conclusive information about the critical behavior of the transition as the possible anisotropic effects can be averaged out [22]. Another important issue is that, in too many cases, the quality of the experimental work from which the critical exponents have been extracted is not good enough to obtain reliable information. As the critical exponents are obtained fitting different experimental sets of data, the quality of the mathematical treatment performed on them are also at the core of this kind of study. It is very important to take these matters into account when comparing literature results.

Table 1
Main universality classes and their critical parameters for magnetic systems [13–16].

Universality class	α	β	γ	δ	A^+/A^-
Mean-field Model	0	0.5	1.0	3.0	–
3D-Ising	0.11	0.3265	1.237	4.79	0.53
3D-XY	−0.014	0.34	1.30	4.82	1.06
3D-Heisenberg	−0.115	0.365	1.386	4.80	1.52

In the particular case of $Pr_{0.5}Sr_{0.5}MnO_3$ and $Nd_{0.5}Sr_{0.5}MnO_3$, there are only a few studies on critical behavior in literature, without much agreement among them. Starting with $Pr_{0.5}Sr_{0.5}MnO_3$, Pramanik et al. [32] studied a polycrystalline sample and they obtained critical exponents $\beta = 0.44$, $\gamma = 1.34$ and $\delta = 4.0$ whose values are between 3D-Heisenberg and Mean-field model, which could be related to a disordered magnet, while Caballero Flores et al. [33] obtained $\beta = 0.394$, $\gamma = 1.44$ and $\delta = 4.651$ with another polycrystalline sample. In this last work these values were attributed to the coexistence of FM and AFM phases as well as to the possible presence of FM clusters in the AFM matrix. A close composition also studied is $Pr_{0.52}Sr_{0.48}MnO_3$ (which has a similar phase diagram but where the transition takes place at a higher temperature), where the obtained values were $\beta = 0.46$, $\gamma = 1.21$ and $\delta = 3.56$ with a single crystal. These values were explained within the framework of a 2D-Heisenberg type long range model [31]; the authors justified the 2D character of the long range interaction on the presence of the FM double exchange interaction in the *bc* planes while the AFM superexchange interaction lies along the *a* axis.

Turning our attention to $Nd_{0.5}Sr_{0.5}MnO_3$, Ventakesh et al. [34] obtained $\beta = 0.5$, $\gamma = 1.02$ and $\alpha = 0.12$ studying a single crystal. The first two exponents correspond nicely to a mean field model while the third one is exactly the value for the anisotropic Ising model; in spite of this contradiction between a long-range model and a short-range one, their conclusion was, surprisingly, that the result was in-between the 3D-Heisenberg model and the mean field one. Krishnamurty et al. [35] studied the muon-spin relaxation in a single crystal and obtained the static critical exponents $\beta = 0.33$, $\gamma = 1.24$ (which are quite close to those for the 3D-Ising model) and the dynamical critical exponent $z = 2.0$, which is close to the theoretical one of a dipolar ferromagnet (model A) (for an isotropic Heisenberg model it is 5/2 while for the anisotropic ferromagnet (model C) it is 2.157) [36]. Finally, Rosenkrantz et al. [37] studied small-angle neutron scattering on a single crystal and they extracted the critical parameter $\nu = 0.61$ which, after the theoretical work by Jasnow et al. [38], corresponds to the 3D-Ising model though the authors do not elaborate on that.

From the information exposed in the two previous paragraphs, it is clear that there are severe contradictions concerning the universality classes to which $Pr_{0.5}Sr_{0.5}MnO_3$ and $Nd_{0.5}Sr_{0.5}MnO_3$ belong. Since any universality class is a reflection of the particular Hamiltonian needed to describe the physical mechanisms responsible for the phase transition under study, its precise attribution gives valuable information about the magnetism of these samples, which is not completely settled yet. Deviations from a double exchange mechanism, magnetocrystalline anisotropies, long or short range mechanisms, disorder … will give different sets of critical exponents; nevertheless, in order to unambiguously settle this question, it is necessary to perform comprehensive studies with which as many critical exponents as possible are obtained, performing high quality experimental measurements, preferable with single crystals. This is the main aim of this study which will also contribute to establish the evolution of the magnetic properties of the series $R_{1-x}Sr_xMnO_3$ by means of the changes in their critical

exponents.

2. Samples and experimental techniques

An important issue when studying critical behavior is to do it on appropriate samples. It is well known that single crystals are ideal for that kind of study as polycrystalline samples present a strong smearing in the phase transitions, making it difficult to evaluate the critical parameters. Single crystals $Pr_{0.5}Sr_{0.5}MnO_3$ and $Nd_{0.5}Sr_{0.5}MnO_3$ were grown by the floating zone technique using a 2 mirror optical furnace, in air, using growth speeds of around 4–6 mm/h [39]. Crystal quality and orientation were determined using the x-ray Laue diffraction technique. The crystals were cut from the as-grown boule in the shape of plane parallel slabs of around 500 μm thickness for the measurements.

Magnetization (M) measurements have been carried out in a VSM (Vibrating Sample Magnetometer) by Cryogenic Limited under external applied magnetic fields H_a ranging from 0 to 80 kOe. Isotherms were collected over a range of about ±15K around T_C ($\Delta T = 1$K) in order to adequately cover the critical region. The magnetic susceptibility was measured with AC Measurement System Option in PPMS (Physical Properties Measurement System) by Quantum Design in order to calculate the demagnetization factors.

Concerning specific heat, results already published in literature [40–42] show that this thermal property presents very broad and small peaks in both cases (indeed, more a bulge over the background than a peak), from which it is not possible to extract a reliable value of the critical exponent α. Nevertheless, we have also used a high resolution ac photopyroelectric calorimeter in the back detection configuration, with which many critical behavior studies have been performed (see the review by Zammit et al. [43]), to obtain thermal diffusivity and specific heat, which are both useful to obtain α. But we have confirmed that the phase transitions in these thermal properties are signaled as too broad and small peaks, with no marked features, from where no reliable quantitative information can be extracted on the critical exponents. That's why thermal measurements are not added to the magnetic ones to perform this study.

3. Experimental results and fittings

Fig. 1 shows the magnetization of both samples as a function of temperature under an applied field of 100 Oe where the ferromagnetic transitions are displayed. The transition temperatures obtained from these measurements are $T_C \approx 249.5$K for $Pr_{0.5}Sr_{0.5}MnO_3$ and $T_C \approx 251.8$K for $Nd_{0.5}Sr_{0.5}MnO_3$. These temperatures are in agreement with literature [33–35]. Concerning the particular shape of the magnetization for $Pr_{0.5}Sr_{0.5}MnO_3$, it is also in agreement with previously published results, where the magnetization grows from the value it attains at the antiferromagnetic to ferromagnetic transition at low temperature till T_C is reached. In polycrystalline samples with applied high fields, the shape is much more rounded [2,32] whereas in low fields it is reasonably sharp [44]. Ours is probably sharper because the field is even lower and it is a single crystal sample. The particular evolution of magnetization with temperature between T_N and T_C has been studied in detail and interpreted as being the result of the presence of antiferromagnetic clusters coexisting with the ferromagnetic phase [44].

In this section, the full scaling analysis will be presented for each sample. In all cases, the magnetic field H_a has been corrected for demagnetization effects to extract the internal field using the relation $H_i = H_a - NM$ where M is the measured magnetization and N the demagnetization factor. N has been obtained from ac susceptibility measurements following the method given by Jiang et al. [45] and the so obtained H_i has been used for the scaling analysis. The demagnetization factors so obtained have been $N = 21.83$ gOe/emu for $Pr_{0.5}Sr_{0.5}MnO_3$ and $N = 22.74$ gOe/emu for $Nd_{0.5}Sr_{0.5}MnO_3$.

3.1. $Pr_{0.5}Sr_{0.5}MnO_3$

Fig. 2a contains the standard Arrott Plot, where M^2 is represented as a function of H/M (in what follows, H will always be the

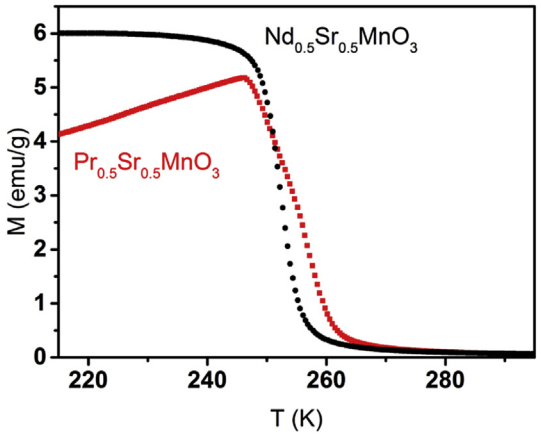

Fig. 1. Magnetization as a function of temperature measured in a field-cooled state using a magnetic field of 100 Oe for $Pr_{0.5}Sr_{0.5}MnO_3$ (■) and $Nd_{0.5}Sr_{0.5}MnO_3$ (●).

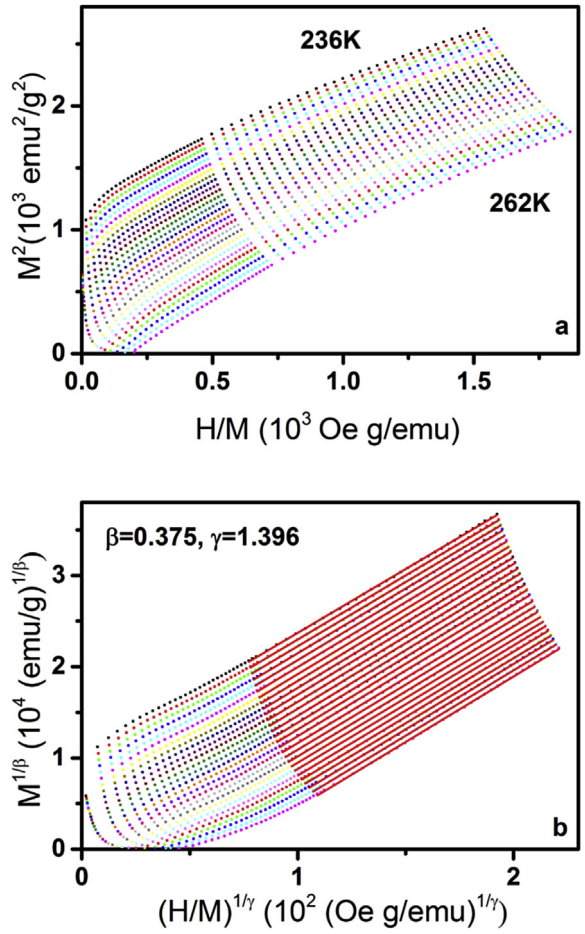

Fig. 2. (a) Arrott Plot of isotherms collected around T_C for $Pr_{0.5}Sr_{0.5}MnO_3$. (b) Optimized Modified Arrott Plot after the iteration procedure.

internal field H_i) for isotherms in the temperature range 236–262 K. If long-range interactions were responsible for the ferromagnetic transition, there would be a linear behavior at high fields, which clearly is not the case. As all curves present a downward slope, a non-mean field behavior is present in this case. Following the Banerjee criterion [46], the positive slope of the curves confirms the second order character of the transition. To establish the value of the critical exponents and thus the class of universality to which $Pr_{0.5}Sr_{0.5}MnO_3$ might belong, we have turned our attention to the Modified Arrott Plots (MAP), plotting $M^{1/\beta}$ versus $(H/M)^{1/\gamma}$. As starting trial values, we have taken the ones corresponding to the well known Ising ($\beta = 0.3265$, $\gamma = 1.2372$) and Heisenberg ($\beta = 0.365$, $\gamma = 1.386$) models. Linear fittings of the experimental points at high field values give us quantitative information when comparing their slopes for each universality class. In both cases, there is an apparent linearity. The deviation of the slopes with respect to the average value goes from −6.7% to +4.6% for the Ising class, while the range is (−1.1%, +0.9%) for the Heisenberg exponents. Thus, the Heisenberg exponents have been taken as the starting point from which an iterative process has been carried out [32]: A linear extrapolation of the isotherms has been taken from the high field values to extract $(M_S)^{1/\beta}$ and $(\chi_0^{-1})^{1/\gamma}$ as an intercept on $M^{1/\beta}$ and $(H/M)^{1/\gamma}$ axis, respectively. These values of $M_S(T)$ and $\chi_0^{-1}(T)$ have been independently fitted to Eqs. (1) and (2), respectively, thus extracting new values of β and γ. The process is repeated till convergence is reached and the best values of β, γ and T_C which give the best parallelism are obtained, which in this case are $\beta = 0.375 \pm 0.004$ and $\gamma = 1.396 \pm 0.019$ (the MAP corresponding to these values is shown in Fig. 2b). The so obtained $M_S(T)$ and $\chi_0^{-1}(T)$ are plotted as a function of temperature in Fig. 3, whose fit to Eq. (1) gives $\beta = 0.376 \pm 0.003$, $T_C = 248.32 \pm 0.02$ K and to Eq. (2) gives $\gamma = 1.403 \pm 0.021$, $T_C = 248.21 \pm 0.12$ K. Both values (β, γ) are only slightly higher than the Heisenberg theoretical values (see Table 1).

As the next step in the scaling analysis, we have followed the Kouvel Fisher method to determine more accurately β, γ and T_C [47]. After this method, both $M_S(dM_S/dT)^{-1}$ and $\chi_0^{-1}(d\chi_0^{-1}/dT)^{-1}$ have a linear behavior with respect to T, with slopes $1/\beta$ and $1/\gamma$, respectively. One of the advantages of this method is that the value of the critical temperature is not introduced *a priori* but extracted from the intercept of the straight fitted lines on the temperature axis. The Kouvel Fisher plot is shown in Fig. 4. The critical parameters obtained are $\beta = 0.385 \pm 0.005$, $T_C = 248.39 \pm 0.04$ K, $\gamma = 1.378 \pm 0.006$, $T_C = 248.33 \pm 0.15$ K. It is worth remarking how

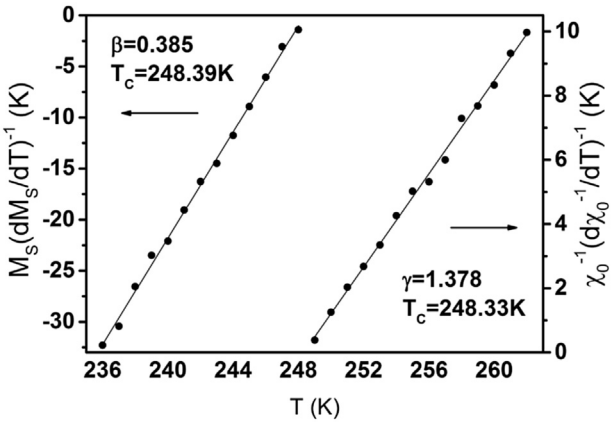

Fig. 4. Kouvel Fisher plot of spontaneous magnetization (left) and inverse of initial susceptibility (right) for $Pr_{0.5}Sr_{0.5}MnO_3$. The straight lines are linear fits, from which T_C and the critical exponents are obtained.

modified Arrott Plots and Kouvel Fisher method give close values of all critical parameters, confirming the robustness of the results.

After Eq. (3), the critical exponent δ can be extracted from the fitting of the critical isotherm to be compared with the values obtained from the scaling law Eq. (5). Fig. 5 shows the critical isotherm at $T = 248$K in log-log scale and a straight line is obtained at high fields, in agreement with theory; its slope is δ. In this particular case, the fitting gives $\delta = 4.72 \pm 0.01$ while the values extracted using Eq. (5) from MAP is 4.73 ± 0.04 and Kouvel-Fisher method 4.58 ± 0.06. So there is a strong coherence among the different results. As a summary, the exponents so obtained are listed in Table 2.

The last confirmation of the validity of the results obtained so far would come from the equation of state Eq. (4) if it were fulfilled with the obtained critical exponents. Fig. 6 shows how all results collapse into two different branches, below and above T_C. This is generally taken as the most severe test for proper scaling.

The conclusion of this section is that the obtained critical exponents β and γ (see Table 2) are slightly bigger than the ones corresponding to the isotropic Heisenberg model ($\beta_{Heis} = 0.365$, $\gamma_{Heis} = 1.386$) while δ is slightly smaller ($\delta_{Heis} = 4.80$).

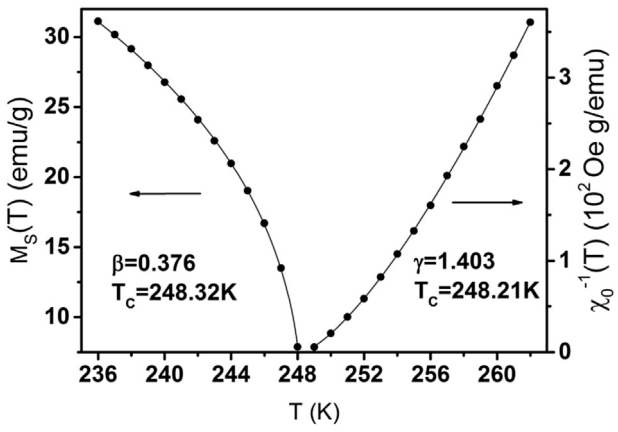

Fig. 3. Spontaneous magnetization (left) and inverse of initial susceptibility (right) vs temperature for $Pr_{0.5}Sr_{0.5}MnO_3$ as obtained from the optimized Modified Arrott Plot. The solid curves correspond to the fits to Eqs. (1) and (2), as explained in the text.

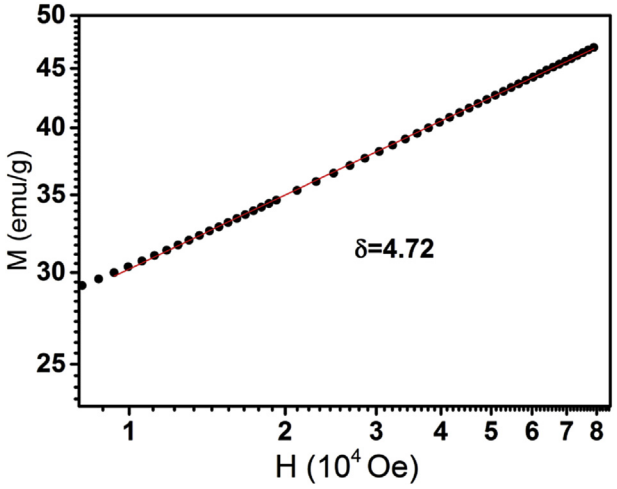

Fig. 5. M vs H plot in a log-log scale collected at $T = 248$ K ($\approx T_C$) for $Pr_{0.5}Sr_{0.5}MnO_3$. The straight line is the linear fit from which the exponent δ is obtained.

Table 2
Values of the obtained critical exponents and parameters β, γ, and δ.

Material	Technique	β	γ	δ
$Pr_{0.5}Sr_{0.5}MnO_3$	Modified Arrott Plot	0.376 ± 0.003	1.403 ± 0.021	4.73 ± 0.04[a]
	Kouvel-Fisher Method	0.385 ± 0.005	1.378 ± 0.006	4.58 ± 0.06[a]
	Critical Isotherm			4.72 ± 0.01
$Nd_{0.5}Sr_{0.5}MnO_3$	Modified Arrott Plot	0.323 ± 0.004	1.201 ± 0.019	4.71 ± 0.10[a]
	Kouvel-Fisher Method	0.322 ± 0.006	1.210 ± 0.023	4.76 ± 0.14 [a]
	Critical Isotherm			4.77 ± 0.01

[a] Calculated from Eq. (5) $\delta = 1 + \gamma/\beta$.

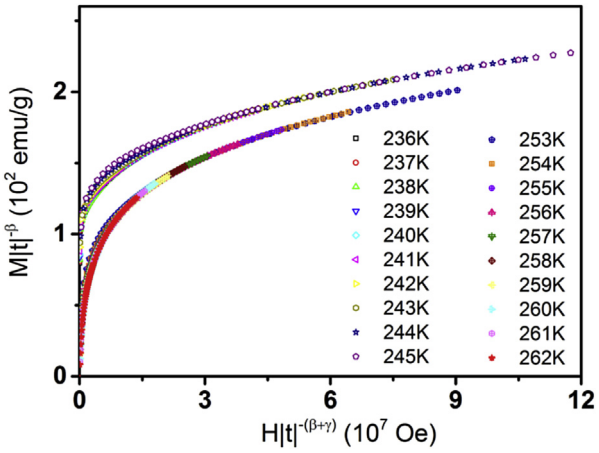

Fig. 6. The renormalized magnetization plotted as a function of the renormalized field following Eq. (4) for $Pr_{0.5}Sr_{0.5}MnO_3$. All data collapse in two separate branches, one above and one below T_C.

3.2. $Nd_{0.5}Sr_{0.5}MnO_3$

An equivalent analysis to the one performed on $Pr_{0.5}Sr_{0.5}MnO_3$ has been carried out with $Nd_{0.5}Sr_{0.5}MnO_3$. Fig. 7a contains the standard Arrott Plot for isotherms in the temperature range 238–262 K. Again, a mean field model does not describe well the critical behavior of this transition, which is confirmed as a second order one by the positive slope of the curves. When taking the Heisenberg and Ising exponents as trial values for a Modified Arrott Plot (MAP), the linear fittings of the experimental points at high field values give a better parallelism for the Ising class than for the Heisenberg one. The deviation of the slopes with respect to the average value is (−7.6% to +6%) for Heisenberg exponents while it is (−2.8% to +1.4%) for the Ising case. Thus, the same rigorous iterative process has been carried out starting with the Ising values. The values for which the best parallelism is found are $\beta = 0.324 \pm 0.004$ and $\gamma = 1.218 \pm 0.023$ and this is shown in Fig. 7b. The values of $M_S(T)$ and $\chi_0^{-1}(T)$ obtained from that graph are plotted as a function of temperature in Fig. 8, whose fit to Eq. (1) gives $\beta = 0.323 \pm 0.004$, $T_C = 250.35 \pm 0.04$ K and to Eq. (2) gives $\gamma = 1.201 \pm 0.019$, $T_C = 250.32 \pm 0.10$ K. Both values are quite close to the Ising theoretical values.

Fig. 9 shows the Kouvel Fisher plots, from whose fittings the critical parameters $\beta = 0.322 \pm 0.006$, $T_C = 250.30 \pm 0.08$ K, $\gamma = 1.210 \pm 0.023$, $T_C = 250.34 \pm 0.18$ K are obtained. It is worth remarking how modified Arrott Plots and Kouvel Fisher method give again close values of all critical parameters, confirming the robustness of the results.

Fig. 10 shows the critical isotherm at $T = 250$ K in log-log scale, which gives a straight line of slope δ. In this particular case, the fitting gives $\delta = 4.77 \pm 0.01$ while the values extracted using Eq. (5) from MAP is 4.71 ± 0.10 and Kouvel-Fisher method 4.76 ± 0.14. So

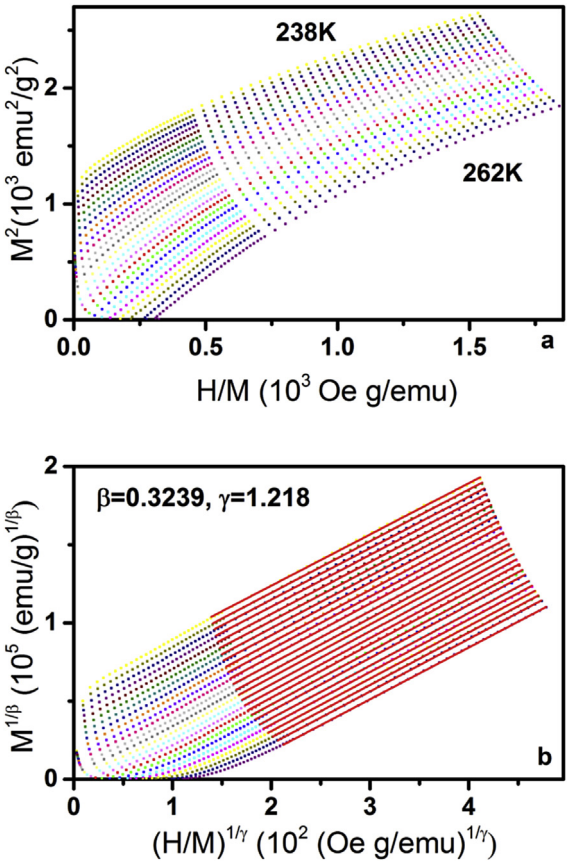

Fig. 7. (a) Arrott Plots of isotherms collected around T_C for $Nd_{0.5}Sr_{0.5}MnO_3$. (b) Optimized Modified Arrott Plots after the iteration procedure.

there is a strong coherence among the different results. All the critical exponents found are listed in Table 2.

Finally, Fig. 11 shows the plot corresponding to the equation of state Eq. (4) with those critical exponents found. All results collapse perfectly well into two different branches, below and above T_C.

Thus, in this second case, the critical exponents β, γ and δ (see Table 2) agree with the anisotropic Ising model, within the experimental error.

4. Discussion

The experimental results presented in the previous section unambiguously ascribe the paramagnetic to ferromagnetic phase transition in $Nd_{0.5}Sr_{0.5}MnO_3$ to the 3D-Ising universality class, which implies strong anisotropic properties, deviating from the description proposed by the DE mechanism. This is not really surprising taking into account the different studies published in literature which account for different magnetocrystalline

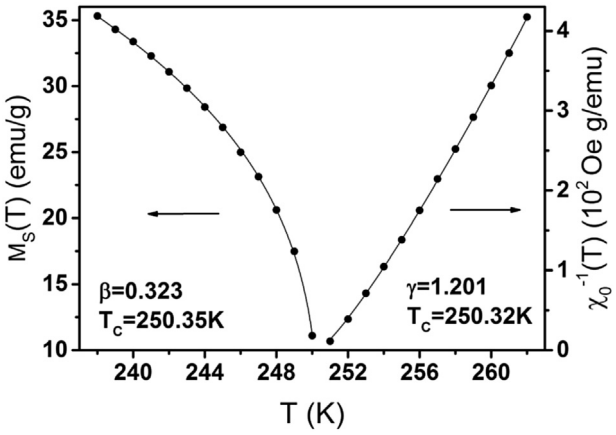

Fig. 8. Spontaneous magnetization (left) and initial susceptibility (right) vs temperature for $Nd_{0.5}Sr_{0.5}MnO_3$ as obtained from the optimized Modified Arrott Plot. The solid curves correspond to the fits to Eqs. (1) and (2), as explained in the text.

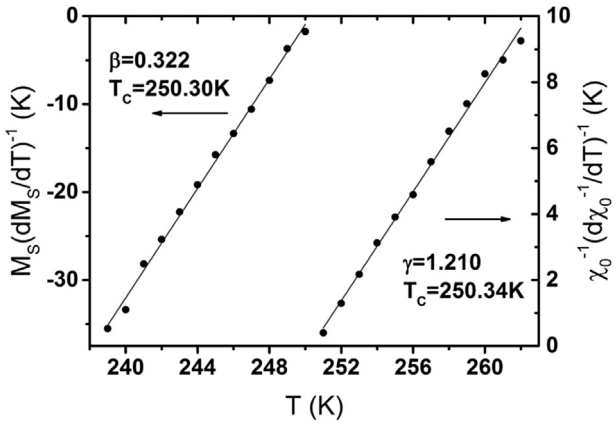

Fig. 9. Kouvel Fisher plot of spontaneous magnetization (left) and inverse of initial susceptibility (right) for $Nd_{0.5}Sr_{0.5}MnO_3$. The straight lines are linear fits, from which T_C and the critical exponents are obtained.

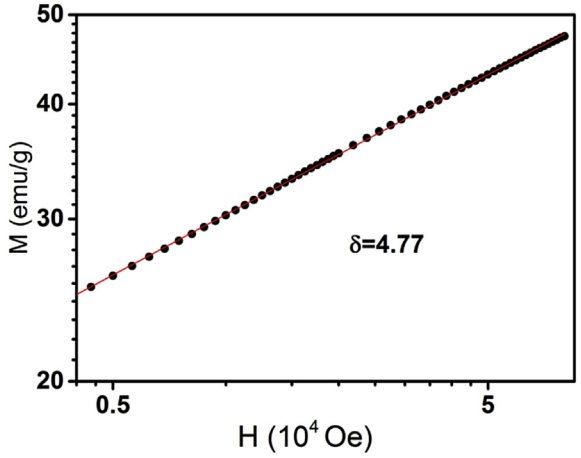

Fig. 10. M vs H plot in a log-log scale collected at $T = 250$ K ($\approx T_C$) for $Nd_{0.5}Sr_{0.5}MnO_3$. The straight line is the linear fit from which the exponent δ is obtained.

anisotropies. The studies on spin dynamics developed by a Japanese group [3,4,48] have proved that there are two types of spin fluctuations: quasielastic isotropic diffuse scattering and dynamical

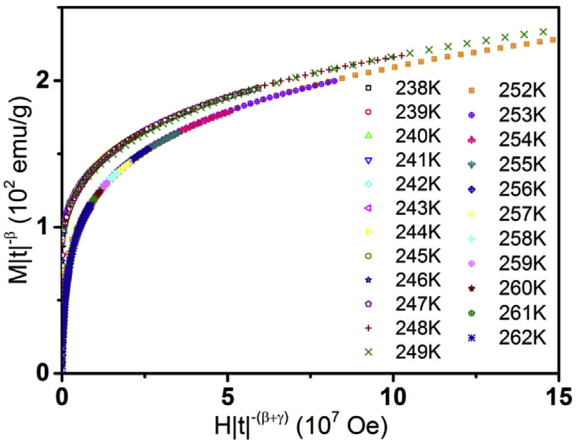

Fig. 11. The renormalized magnetization plotted as a function of the renormalized field following Eq. (4) for $Nd_{0.5}Sr_{0.5}MnO_3$. All data collapse in two separate branches, one above and one below T_C.

anisotropic spin fluctuations; the latter posses *A*-type AFM spin correlations in their FM states. This anisotropic behavior is attributed to the orbital ordering in these systems, which arises from a Jahn-Teller distortion which induces the $d_{x^2-y^2}-$ type orbital-order. This is in agreement with the results of Kiryukhin et al. [49] who, based on X-ray scattering studies, found a correlated anisotropic lattice distortion in the FM and PM phase which are associated with local regions of layered orbital and magnetic order. They conclude that short-range structural correlations associated with local regions of orbital and magnetic order play an important role in this material. Another anisotropic behavior has also been found both in the AFM and FM phases when measuring the optical conductivity spectra, incompatible with typical DE ferromagnetic-metallic phases [50]. Finally, recent measurements with inelastic neutron-scattering experiments on $Nd_{0.5}Sr_{0.5}MnO_3$ have also shown deviations from the isotropic description [51], as they found a spin-wave dispersion which could be described by a Heisenberg model plus weak additional intensities near the zone boundaries over a wide energy band. All of these mechanisms justify the deviation from the Heisenberg universality class and the need for an anisotropic model such as the 3D-Ising to describe the critical behavior.

Finally, it is worth pointing out that the critical parameters found in this study also agree with the ones obtained by means of muon-spin relaxation [35] and small-angle neutron diffraction [37] already mentioned in the introduction, all of them in compliance with the 3D-Ising model.

Now, if we turn our attention to the critical exponents obtained for $Pr_{0.5}Sr_{0.5}MnO_3$, we see that the values of the critical parameters β and γ are slightly bigger than the ones corresponding to the isotropic Heisenberg model (compare Table 1 with Table 2, the differences in γ are within the experimental error, the differences in β are a little bit out of it). Nevertheless, the difference is not relevant enough to assign them to another universality class such as a separate class or a 2D-model as it has been claimed before [31,32] (though the work in Ref. [31] is for a slightly different composition). They are quite similar to the ones found by Caballero Flores et al. [33] studying the magnetocaloric effect. The question is: what could we expect from the knowledge on the magnetism in $Pr_{0.5}Sr_{0.5}MnO_3$ and the comparison with $Nd_{0.5}Sr_{0.5}MnO_3$? While in the second compound a coexistence of AFM phase in the FM region has been found (between T_C and T_N) [3], this has not been proved in the first one, as phase coexistence has only been found at low temperature, starting below 148K [10]. The same Japanese group who studied $Nd_{0.5}Sr_{0.5}MnO_3$ spin dynamics also turned their

attention to $Pr_{0.5}Sr_{0.5}MnO_3$ [3,4,47] and they found, indeed, an anisotropic behavior as well but when they compared the spin dynamics of both systems they found that the deviations in the spin wave dispersions in the FM state from what would be expected under the DE model are much more important for the Nd compound than for the Pr one [3]. The only other work in which possible anisotropies have been studied in $Pr_{0.5}Sr_{0.5}MnO_3$ is the one by Tobe et al. [50] on optical conductivity spectra and they found anisotropies as in the case of $Nd_{0.5}Sr_{0.5}MnO_3$. So the conclusions that we can gather from these works is that, if there were to be any deviation from the DE (Heisenberg model), it should be in the same direction as in the case of $Nd_{0.5}Sr_{0.5}MnO_3$ but attenuated because the physical mechanisms which could give rise to anisotropies are less important in $Pr_{0.5}Sr_{0.5}MnO_3$. As for the reasons why we have obtained different parameters than those found in Refs. [32], that study was performed on a polycrystalline sample while in this work it is a single crystal; besides, in their case, they were not able to satisfactorily interpret the nature of their results. From our study we can conclude that the anisotropies observed and published in literature are not important enough so as to make the system deviate from the isotropic behavior and that's the reason why we obtain so neatly Heisenberg values for the critical parameters.

5. Conclusions

A complete and detailed critical behavior study of the paramagnetic to ferromagnetic transition in $Pr_{0.5}Sr_{0.5}MnO_3$ and $Nd_{0.5}Sr_{0.5}MnO_3$ has been performed by means of magnetic techniques in order to independently extract the critical exponents β, γ and δ. In each case the values of these exponents match among them; in the particular case of $Nd_{0.5}Sr_{0.5}MnO_3$, they correspond to the 3D-Ising universality class, indicating that the spin-dynamics anisotropy present in the system is strong enough so as to make it clearly deviate from the simple double exchange description (isotropic Heisenberg model). On the contrary, the critical parameters found for $Pr_{0.5}Sr_{0.5}MnO_3$ agree nearly perfectly with the 3D-Heisenberg model, confirming that the spin-dynamics anisotropy is indeed of lesser importance and that an isotropic description based on the DE mechanism is still valid for this material.

Acknowledgments

This work have been supported by Gobierno Vasco (grant IT619-13), and UPV/EHU (grant UFI11/55). Work at the University of Warwick was supported by EPSRC, UK (grant EP/M028771/1). The authors thank for technical and human support provided by SGIker of UPV/EHU.

References

[1] R. Kajimoto, H. Yoshizawa, H. Kawano, H. Kuwahara, Y. Tokura, K. Ohoyama, M. Ohashi, Phys. Rev. B 60 (1999) 9506.
[2] C. Martin, A. Maignan, M. Hervian, B. Raveau, Phys. Rev. B 60 (1999) 12191.
[3] H. Kawano-Furukawa, R. Kajimoto, H. Yoshizawa, Y. Tomioka, H. Kuwahara, Y. Tokura, Phys. Rev. B 67 (2003) 174422.
[4] H. Kawano, R. Kajimoto, H. Yoshizawa, Y. Tomioka, H. Kuwahara, Y. Tokura, Phys. Rev. Lett. 78 (1997) 4253.
[5] M. Pattabiraman, P. Murugaraj, G. Rangarajan, C. Dimitropoulos, J.Ph. Ansermet, G. Papavassiliou, G. Balakrishnan, D.McK. Paul, M.R. Lees, Phys. Rev. B 66 (2002) 224415.
[6] C. Ritter, R. Mahendiran, M.R. Ibarra, L. Morellon, A. Maignan, B. Raveau, C.N.R. Rao, Phys. Rev. B 61 (2000) R9229.
[7] J.P. Joshi, A.K. Sood, S.V. Bhat, S. Parashar, A.R. Raju, C.N.R. Rao, J. Magn. Magn. Mater. 279 (2004) 91.
[8] V.T. Dovgii, A.I. Linnik, V.I. Kamenev, V.K. Prokopemko, V.I. Mikhailov, V.A. Khokhlov, A.M. Kadomtseva, T.A. Linnik, N.V. Davydeiko, G.G. Levchenko, Tech. Phys. Lett. 34 (2008) 1044.
[9] J. Geck, D. Bruns, C. Hess, R. Klingeler, P. Reutler, M.v. Zimmermann, S.-W. Cheong, B. Büchner, Phys. Rev. B 66 (2002) 184407.
[10] A.K. Pramanik, R. Ranjaan, A. Banerjee, J. Magn. Magn. Mater. 325 (2013) 29.
[11] N. Furukawa, Y. Motome, Appl. Phys. A 74 (2002) S1728.
[12] H.E. Stanley, Introduction to Phase Transitions and Critical Phenomena, Oxford University Press, 1971.
[13] R. Guida, J. Zinn-Justin, J. Phys. A Math. Gen. 31 (1998) 8103.
[14] M. Campostrini, M. Hasenbusch, A. Pelisseto, P. Rossi, E. Vicari, Phys. Rev. B 63 (2001) 214503.
[15] M. Campostrini, M. Hasenbusch, A. Pelisseto, P. Rossi, E. Vicari, Phys. Rev. B 65 (2002) 144520.
[16] M. Hasenbusch, Phys. Rev. B 82 (2010) 174434.
[17] Ch. V. Mohan, M. Seeger, H. Kronmüller, P. Murugaraj, J. Maier, J. Magn. Magn. Mater. 183 (1998) 348.
[18] S.E. Lofland, V. Ray, P.H. Kim, S.M. Bhagat, M.A. Manheimer, S.D. Tyagi, Phys. Rev. B 55 (1997) 2749.
[19] J. Fan, L. Pi, L. Zhang, W. Tong, L. Ling, B. Hong, Y. Shi, W. Zhang, D. Lu, Y. Zhang, Appl. Phys. Lett. 98 (2011) 1072508.
[20] R. Ventakesh, M. Pattabiraman, S. Angppane, G. Rangarajan, K. Sethupathi, J. Karatha, M. Fecioru-Morariu, R.M. Ghadimi, G. Guntherodt, Phys. Rev. B 75 (2007) 224415.
[21] K. Gosh, C.J. Lobb, R.L. Greene, S.G. Karabashev, D.A. Shulyatev, A.A. Arsenov, Y. Mukovskii, Phys. Rev. Lett. 81 (1998) 4740.
[22] S. Röβler, H.S. Nair, U.K. Röβler, C.M.N. Kumar, S. Elizabeth, S. Wirth, Phys. Rev. B 84 (2011) 184422.
[23] A. Oleaga, A. Salazar, D. Prabhakaran, A.T. Boothroyd, Phys. Rev. B 70 (2004) 184402.
[24] D. Kim, B.L. Zink, F. Hellman, J.M.D. Coey, Phys. Rev. B 65 (2002) 214424.
[25] A. Oleaga, A. Salazar, K. Kuwahara, Phys. B 378–380 (2006) 512.
[26] P. Lin, S.H. Chun, M.B. Salamon, Y. Tomioka, Y. Tokura, J. Appl. Phys. 87 (2000) 5825.
[27] A. Oleaga, A. Salazar, M. Ciomaga Hatnean, G. Balakrishnan, Phys. Rev. B 92 (2015) 024409.
[28] T.A. Ho, T.D. Thanh, Y. Yu, D.M. Tartarovsky, T.O. Ho, P.D. Thang, A.T. Lee, T.L. Phan, S.C. Yu, J. Appl. Phys. 17 (2015) 17D122.
[29] W. Jiang, X. Zhou, G. Williams, Y. Mukovskii, R. Privenzentsev, J. Phys. Condens. Matter 21 (2009) 415603.
[30] P.M.G.L. Ferreira, J.A. Souza, J. Phys. Condens. Matter 23 (2011) 226003.
[31] Sk Sabyasachi, A. Bhattacharayya, S. Majumdar, S. Giri, T. Chatterji, J. Alloys Compd. 577 (2013) 165.
[32] A.K. Pramanik, A. Banerjee, Phys. Rev. B 79 (2009) 214426.
[33] R. Caballero-Flores, N.S. Bingham, M.H. Phan, M.A. Torija, C. Leighton, V. Franco, A. Conde, T.L. Phan, S.C. Yu, H. Srikanth, J. Phys. Condens. Matter 26 (2014) 286001.
[34] R. Ventakesh, R. Nirmala, G. Rangarajan, S.K. Malik, V. Sankaranarayanan, J. Appl. Phys. 99 (2006) 08Q311.
[35] V.V. Krishnamurty, I. Watanabe, K. Nagamine, H. Kuwahara, Y. Tokura, Phys. Rev. B 61 (2000) 4060.
[36] H. Hohenemser, N. Rosov, A. Kleinhammes, Hyperfine Interact. 49 (1989) 267.
[37] S. Rosenkranz, R. Osborn, J.F. Mitchell, U. Geiser, J. Ku, A.J. Schultz, D.M. Young, Phys. B 241 (1998) 448.
[38] D. Jasnow, M. Wortis, Phys. Rev. 176 (1968) 739.
[39] A.J. Campbell, G. Balakrishnan, M.R. Lees, D.McK. Paul, G.J. McIntyre, Phys. Rev. B 55 (1997) R8622.
[40] B. Roy, A. Poddar, S. Das, E. Gmelin, J. Alloys Compd. 326 (2000) 317.
[41] A.G. Gamzatov, A.M. Aliev, Sh.B. Abdulvagidov, A.B. Batdalov, O.Y. Gorbenko, A.R. Kaul, Phys. B 395 (2007) 151.
[42] J. Lopez, O.F. de Lima, J. Appl. Phys. 94 (2003) 4395.
[43] U. Zammit, M. Marinelli, F. Mercuri, S. Paoloni, F. Scudieri, Rev. Sci. Inst. 82 (2011) 121101.
[44] A.K. Pramanik, A. Banerjee, J. Phys. Condens. Matter 20 (2008) 275207.
[45] W. Jiang, X.Z. Zhou, G. Williams, Y. Mukovskii, K. Glazyrin, Phys. Rev. B 78 (2008) 144409.
[46] S.K. Banerjee, Phys. Lett. 12 (1964) 16.
[47] J.S. Kouvel, M.E. Fisher, Phys. Rev. 136 (1964) A1626.
[48] H. Yoshizawa, R. Kajimoto, H. Kawano, J.A. Fernandez-Baca, Y. Tomioka, H. Kuwahara, Y. Tokura, Mater. Sci. Eng. B 63 (1999) 125.
[49] V. Kiryukhin, B.G. Kim, T. Katsufuji, J.P. Hill, S.-W. Cheong, Phys. Rev. B 63 (2001) 144406.
[50] K. Tobe, T. Kimura, Y. Tokura, Phys. Rev. B 69 (2004) 014407.
[51] H. Ulbrich, F. Krüger, A.A. Nugroho, D. Lamago, Y. Sidis, M. Braden, Phys. Rev. B 84 (2011) 094453.